Evaluating Demand Response in the Presence of Solar PV: Distribution Grid Perspective

Sarmad Hanif[1,2*], Tobias Massier[1‡], Thomas Hamacher[3§], Thomas Reindl[2¶]
[1]TUM CREATE Limited, Singapore 138602
[2]Solar Energy Research Institute of Singapore (SERIS), National University of Singapore (NUS), Singapore 117574
[3]Technical University of Munich (TUM), Garching 85748, Germany
*sarmad.hanif@tum-create.edu.sg, ‡tobias.massier@tum-create.edu.sg,
§thomas.hamacher@tum.de, ¶thomas.reindl@nus.edu.sg

***Abstract*—Flexible load operators are particularly interested in monetary transactions of demand response (DR). However, the integration of the DR scheme into the distribution network results in modification of power flows, which has to be managed by the distribution system operator (DSO). Hence, a coordination must be achieved between these two entities to comply with their individual constraints and objectives. With the integration of highly distributed and variable renewable energy, achieving this coordination becomes an even more important task. In this paper, an optimization-based generic model is presented for evaluating DR in the presence of solar photovoltaic (PV) and flexible loads. The integrated optimal pricing methodology is obtained from the developed framework, which takes into account operational conditions of the distribution grid and flexible loads. The economic and operational efficiency of the DR strategy is evaluated in the presence of (1) various pricing structures and (2) available network topologies. Case studies are performed using a validated building model and actual solar irradiation measurements on a benchmark distribution network. For comparison, liberalized market settings of the National Electricity Market of Singapore (NEMS) are adopted in this paper.**

***Index Terms*—Flexible Demand, Buildings, Renewable Energies, Distribution Grids.**

I. Introduction

DR strategies aiming to achieve controllability in electric demand help power systems become more efficient and resilient [1], [2]. Furthermore, with the advent of renewable energies and liberalized markets, controllable demand has also shown the potential to help integrate variable renewable energies into the market [3], [4]. Hence, in the near future, it is expected that flexible demand might play an integral role in the efficient operation of the power system.

Buildings as flexible loads with the combination of solar PV as a renewable energy source have been reviewed in [5]. The reason for studying buildings and solar PV in combination is due to the fact that buildings' energy demand and solar irradiation are positively correlated. Hence, in principle, the co-optimization of both systems has the potential of complementing one another's behavior. Furthermore, in an urban environment with limited ground space, roof-top (building) PV is also becoming a common site. However, a certain amount of controllability in buildings' electricity demand is imperative for carrying out the co-optimization of the whole (PV-building) system. Keeping this in mind, there have already been numerous works to obtain controllable building models. Some of them can be found in [6]–[8]. With regards to applications of these developed models, authors have mostly concentrated on developing DR strategies with cost minimization [6], [7], [9] or providing grid services [10], [11].

Physically, the flexible demand is usually integrated in the electricity distribution grid (medium-low voltage level). Hence, in order to avoid interference in the usual operation, the developed DR strategy must incorporate physical and economical limitations of the distribution grid. With the similar philosophy, in [12], authors proposed methodologies to couple prices and control of various appliances in the future smart distribution system. In particular, authors pushed the idea for the distribution locational marginal price (DLMP). The prime reason for advocating the DLMP was to increase the economic efficiency and operational reliability of the distribution grid. Also, authors in [13]–[15] showed efficient integration of flexible loads and renewable energies in the distribution grid using the DLMP.

According to our knowledge, a gap in the existing literature still exists regarding the technical and economical analysis of distribution grids in the presence of combined scheduling of distributed solar PV and controllable buildings. Hence, in this paper, we analyze the combined effect on the economic and technical limitation of the distribution grid due to the integration of price-responsive buildings and the distributed solar PV. In particular, focus is given to branch flows in the distribution grid and its relation to the energy procurement cost.

The contribution of this paper is twofold. First, the economic efficiency and the distribution grid operation is compared with respect to various pricing structures. This comparison is carried out within the cost minimization framework, achieving a consensus between distribution grid and its underlying flexible consumers. Furthermore, a comparison is also performed between the integrated optimal prices (DLMPs) and the usual pricing structure of the distribution grid. Second, distribution grid's topology and its relationship with the increase in the overall cost of energy procurement is investigated.

Section II explains the modeling procedure for distribution grids. The optimal integrated pricing methodology is

introduced in Section III. The simulation setup and results are presented in Section IV. In the end, conclusion and recommended future works related to this study are provided in Section V.

II. Distribution System Model

This section describes assumptions and models used to conduct simulation in this paper. The grid operation is modeled through optimal power flow (OPF). This means that scheduling of flexible loads and renewable generation is carried out through an optimization problem.

$$\min_{p^*_{i,k}} \sum_{i\in N_k}\sum_{k\in N_t} J_{i,k} \tag{1a}$$

subject to

$$1^T p_{i,k} = 0 \qquad ;\mu_k \tag{1b}$$

$$\sum_{i\in N_i}\sum_{k\in N_t} D\ p_{i,k} \le p_b^{max} \qquad ;\lambda_k^+ \tag{1c}$$

$$\sum_{i\in N_i}\sum_{k\in N_t} -D\ p_{i,k} \le p_b^{max} \qquad ;\lambda_k^- \tag{1d}$$

$$p_{i,k}^{min} \le p_{i,k} \le p_{i,k}^{max} \qquad \forall k\in N_t, \forall i \in N_i \tag{1e}$$

For each load point (LP) ($i \in n_{LP}$) and time step ($k \in N_t$), the multi-period OPF (1a) finds an optimal generation/demand dispatch $p^*_{i,k} \in R^{n_{LP}}$. The OPF is constrained through node balance (1b), branch [(1c), (1d)] and injections limits (1e) of the network. For n_l distribution lines, $D \in \mathbb{R}^{n_l \times n_{LP}}$ is the power transfer distribution matrix, representing the sensitivity of branch flows ($p_b \in R^{n_l}$) to the node injections $p_{i,k}$ in the network. Lagrange multipliers (LMs) $\lambda_k^{+/-} \in \mathbb{R}^{n_l}$ and $\mu_k \in \mathbb{R}^{n_{LP}}$ are associated with branch flows and node balance constraints, respectively.

A. Loss Approximation

The lossless linear OPF in (1) represents a standard procedure for system operators to clear the energy market at the transmission level [16]. However, losses at the distribution level are not ignorable [17]. This is mainly because the distribution grid has a higher resistance and lower voltage level than the transmission grid. Furthermore, including AC load flow equations renders the optimization problem highly non-convex and nonlinear.

To overcome this issue, authors in [18] introduced a piecewise linear approximation of losses in the network. To deal with the exclusivity and adjacency violations, authors also incorporated integers ($w^{b^-}_{s,k}$, $w^{b^+}_{s,k} \in \mathbb{R}^{n_l\times(S+1)}$) in the formulation. Where S is the total number of linear segments used to approximate actual branch angles leaving $\theta^{b^+}_{s,k}$ and entering $\theta^{b^-}_{s,k} \in \mathbb{R}^{n_l\times S}$ the node i at time k.

The nodal loss term $p_{l_{i,k}} \in R^{n_{LP}}$ is approximated using (2a), where $G_b \in R^{n_{LP}\times n_l}$ is the conductance matrix. The set $b_{I,i}$ and $b_{O,i}$ represent branch flows entering and leaving the node i. The slope segment of the piecewise linearized branch flow angle is given by $seg_s \in \mathbb{R}^{n_l\times S}$. constraints [(2c)-(2g)] enforce exclusivity and adjacency condition to the loss approximations in (2a), (2b) (for details see [19]).

$$\begin{aligned} p_{l_{i,k}} &= \sum_{\forall b\in b_{I,i}} 2G_b\Big(\sum_{\forall s\in S} seg_s\cdot\theta^{b^-}_{s,k}\Big) \\ &+ \sum_{\forall b\in b_{O,i}} 2G_b\Big(\sum_{\forall s\in S} seg_s\cdot\theta^{b^+}_{s,k}\Big) \end{aligned} \tag{2a}$$

$$\theta_{b_{I,i}} - \theta_{b_{O,i}} = \sum_{\forall s}\theta^{b^+}_{s,k} - \sum_{\forall s\in S}\theta^{b^-}_{s,k} \tag{2b}$$

$$w^{b^+}_{s+1,k}\cdot\theta^{max}_{s,k} \le \theta^{b^+}_{s,k} \le w^{b+}_{s,k}\cdot\theta^{max}_{s,k} \tag{2c}$$

$$w^{b^-}_{s+1,k}\cdot\theta^{max}_{s,k} \le \theta^{b^-}_{s,k} \le w^{b^-}_{s,k}\cdot\theta^{max}_{s,k} \tag{2d}$$

$$\theta^{b^+}_{s,k} \le \theta^{max}_{s,k} \tag{2e}$$

$$\theta^{b^-}_{s,k} \le \theta^{max}_{s,k} \tag{2f}$$

$$w^{b^-}_{s,k} + w^{b^+}_{s,k} \le 1 \tag{2g}$$

The loss approximation presented in (2) captures ohmic losses of the system indigenously, while keeping the formulation tractable. The mixed-integer formulation does not provide off the shelf LMs of binding constraints. LMs can be obtained from a two step procedure: (1) by solving the problem for optimal segments (integers) and then (2) fixing the obtained segments (integers) and solving the original problem again.

B. Node Injections

For this paper, two types of flexible node injections are assumed: (1) large controllable commercial consumers and (2) distributed roof-top PV. In particular, the mass flow rate of the heating, ventilation and air conditioning is modeled as a flexibility source [11]. The model predicts the temperature of the room x_{z_k} (surrounding walls and the room) as state space function of the HVAC mass flow u_{z_k} and disturbances $\hat{d}_{z_k}$ as:

$$x_{z_{k+1}} = Ax_{z_k} + Bp(u_{z_k}) + E\hat{d}_{z_k}. \tag{3a}$$

The expression of the power flow in the above equation is calculated as:

$$p(u_{z_k}) = p_{\mathrm{heat},k} + p_{\mathrm{fan},k}, \tag{4}$$

$$p_{\mathrm{heat},k} = u_{z_k} c_{\mathrm{p}}(T_{\mathrm{in},z_k} - T_{\mathrm{room},z_k}),\ p_{\mathrm{fan},k} = \frac{u_{z_k}\Delta p}{\rho}. \tag{5}$$

The above presented model is validated against real measurements, and for further insight into the units, dimensions and modeling procedure, readers are referred to [6]. The single room state space model of (3) is augmented by the given number of rooms, floors and buildings of the respective LP of the distribution grid.

$$x_{i,k+1} = Ax_{i,k} + Bp(u_{i,k}) + E\hat{d}_{i,k} \tag{6a}$$

$$p_{flex_{i,k}} = M_{flex}p(u_{i,k}) \tag{6b}$$

$$p^{min}_{flex_{i,k}} \le p_{flex_{i,k}} \le p^{max}_{flex_{i,k}} \tag{6c}$$

The thermal model in (6a) is the augmented version of (3) and represents the modeled building in its respective i^{th} LP. The flexible power injected into the distribution grid is represented by $p_{flex_{i,k}} \in \mathbb{R}^{n_{LP}}$. The matrix $M_{flex} \in \mathbb{R}^{n_{LP}\times n_{flex}}$ maps

the flexible consumption $p(u_{i,k}) \in \mathbb{R}^{n_{flex}}$ for n_{flex} flexible consumers to their respective LPs. The feasible actuator limits are represented in (6c).

The PV generation $p_{pv_{i,k}}$ at i^{th} node is modeled using the translation of total rooftop area covered by the PV system (A_{pv}) and its efficiency (η_{pv}) onto the received irradiation ($u^{irr}_{i,k}$).

$$p_{pv_{i,k}} = M_{pv} u^{irr}_{i,k} A_{pv} \eta_{pv} \tag{7}$$

The matrix M_{pv}, is similar to M_{flex}, but for this case, it maps the total number of PV systems n_{pv} to their respective i^{th} LPs. Option for the flexible consumer exist to consume PV production locally ($p^l_{pv_{i,k}}$) or to purchase it from the grid ($p^g_{flex_{i,k}}$).

$$p_{pv_{i,k}} = p^g_{pv_{i,k}} + p^l_{pv_{i,k}} \tag{8a}$$

$$p_{flex_{i,k}} = p^g_{flex_{i,k}} - p^l_{pv_{i,k}} \tag{8b}$$

Finally, the total injection at the i^{th} node for step k is given as:

$$p_{i,k} = p_{pv_{i,k}} - p_{flex_{i,k}} - p_{fix_{i,k}} - p_{l_{i,k}}. \tag{9}$$

The term $p_{fix_{i,k}}$ is the fixed consumption of LPs. These quantities are estimated based on the historical data. In the end, the full distribution grid OPF (1) is formulated by including constraints for approximating losses (2), flexible loads (6), and renewable generation (8).

III. Integrated Optimal Pricing

For the pricing structure, the setting of wholesale competition is assumed in this paper [20]. This means that most of the energy is purchased by the DSO for its consumers, who is also responsible for the maintenance and power quality of the grid. However, large consumers (based on their registered power rating) can buy energy directly from the wholesale market. One of the example of this setting is the NEMS [21], where larger consumers are given the option to purchase energy through a retailer or directly from the Energy Market Company (EMC) [22]. In general, the considered prices in this paper are: (1) the flat tariff (FT) which is charged by the DSO to small consumers and (2) the energy price (LMP) which is cleared in the market clearing engine at the system operator. The FT is usually decided so that the cost incurred by utilities are recovered in a reasonable time. The LMP on the other hand reflects condition of the power system (usually transmission grid) such as congestion, generation and load levels. Even though the nature of the wholesale market is captured through LMP, it still does not account for the distribution system condition. And in order to capture the maximum capabilities of distributed generation and price-responsive loads, monetary incentives and technical limitations of the distribution grid must be aligned. The DLMP, similar to LMP, is a LM-based pricing methodology. In particular, the DLMP translates relevant OPF constraints as an increase in the overall cost of the system. In this way DLMPs are able to represent internal distribution grid constraints. In order to derive the DLMP, consider the partial Lagrangian of (1) when only branch flow constraints are binding.

$$L(p_{i,k}, \lambda^+_k, \lambda^-_k) = \sum_{i \in N_k} \sum_{k \in N_t} J_{i,k} + (\lambda^+_k - \lambda^-_k)^T (D p_{i,k} - f_l) \tag{10}$$

For time k and node i, the DLMP from the Lagrangian then follows,

$$\lambda_{\mathrm{dlmp}_{i,k}} = \frac{\partial L}{\partial p_{i,k}} = \frac{\partial J_{i,k}}{\partial p_{i,k}} + M^T D^T (\lambda^+_k - \lambda^-_k). \tag{11}$$

The matrix M in (11) translates the flexible node injection $p_{i,k}$ to distribution grid LPs. In (11), one can observe that there are two components dictating the price: (1) the energy prices or LMP, propagating from the transmission grid ($\frac{\partial J_{i,k}}{\partial p_{i,k}}$) and (2) the locational price due to distribution grid's binding constraints (λ^+_k, λ^-_k). Hence, the $\lambda_{\mathrm{dlmp}_{i,k}}$ in (11) reflects both the overall power system and the distribution grid conditions.

Since the locational price is the outcome of the distribution grid's operational and constructional conditions, we cannot model it in advance. On the other hand the LMP is propagated from the market clearing procedure and contains certain properties such as the correlation with the forecast of the demand and renewable energies. These properties can indeed be modeled and included in the objective function, as the cost for energy purchase is minimized in the objective function of the OPF (1a). The rationale behind minimizing the energy cost is that: (1) consumers are only concerned with the monetary incentives and (2) the individual cost optimization problem of each consumer is represented as a subproblem within the overall OPF (1). As a result, the optimal solution acquired by solving the overall problem also ensures a feasible solution for flexible nodes.

The total cost of procuring energy is given by:

$$J_{i,k} = c_{0,k} p_{flex_{i,k}} - f_{0,k} p^g_{pv_{i,k}}. \tag{12}$$

In (12), for each step k, $c_{0,k}$ and $f_{0,k}$ represent cost of purchasing energy from the gird and the revenue for selling PV energy back to the grid, respectively. With the cost function (12) included in the overall optimization problem (1), the resultant optimization problem is a mixed-integer linear program (MILP). However, with the procedure described in Section II-A, MILP can be effectively turned into a linear program. In [14], authors proved that the maximum consensus (global optimal) between the DSO problem and the flexible consumer, is only achieved through quadratic programing. Hence, a quadratic objective function is formulated by introducing a price sensitivity term (β_{flex}) in the energy price and PV feed-in energy (β_{pv}).

$$J_{i,k} = c^T_k p_{quad_{i,k}} + \frac{1}{2} p^T_{quad_{i,k}} B p_{quad_{i,k}} \tag{13}$$

with,

$$c_k = \begin{bmatrix} c_{0,k} \\ -f_{0,k} \end{bmatrix}, \; B = \begin{bmatrix} \beta_{flex} & 0 \\ 0 & \beta_{pv} \end{bmatrix}, \; p_{quad_{i,k}} = \begin{bmatrix} p_{flex_{i,k}} \\ p^g_{pv_{i,k}} \end{bmatrix}.$$

The term β_{flex} represents the relationship of increase in the energy price due to the increase in the demand. Similarly, β_{pv} depicts the decrease in the energy price due to the increase in the renewable feed-in. Interested readers are directed to [13], [23] for more explanations regarding the price sensitivity terms. In (13), one can see that the Hessian (B) is a positive definite matrix. This implies that the resultant optimization is a strictly convex problem, with necessary and sufficient Karush-Kuhn-Tucker conditions [14]. Intuitively, this means that the solution to the cost minimization problem of the OPF and the flexible consumer converges.

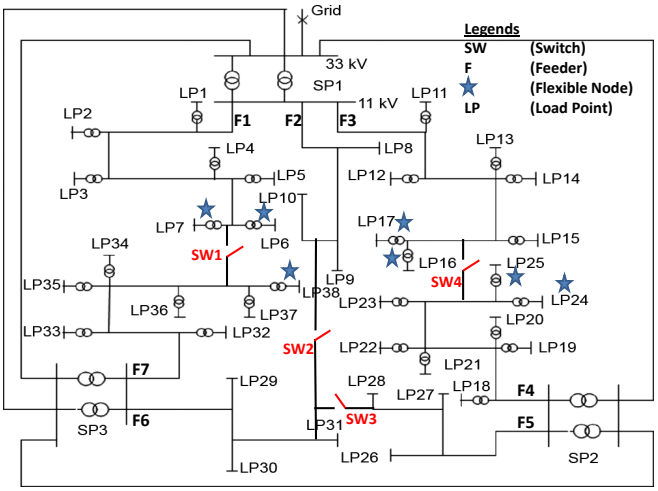

Fig. 1. The RBTS bus 4 system used for the evaluation of the DR strategies [25].

IV. System Setup and Results

The developed DR strategy is evaluated on the Bus 4 distribution network of Roy Billinton Test System (RBTS) (see Fig. 1). The network has seven feeders (F1-7). Four switches (SW1-4) can be used to change the network topology from radial (opened switches) to mesh (closed switches). The renewable energy injection as distributed PV is modeled using the actual irradiation data from the Solar Energy Research Institute of Singapore [24]. It is assumed that the total area covered by the rooftop PV is 400 m^2. The PV system is assumed to be converting the solar irradiation to electric power at the efficiency of 12%. With respect to flexible loads the network originally has 10 consumers connected to each commercial LP [25] (for their location please see Fig. 1). For this paper, it is assumed that each consumer is modeled as a flexible building containing 10 floors and 10 zones per floor. The fixed consumptions for inflexible loads $p_{fix_{i,k}}$ are taken from [25]. The assumed values for β_{pv} and β_{flex} are $1 \cdot 10^6$ and $1 \cdot 10^4$, respectively. For approximating losses, it is assumed that the branch flow angle is divided into 15 segments. The energy price is obtained from the EMC [22].

A. Price Comparison

The above mentioned simulation setup in a radial configuration (SW1-4 open) is simulated for three types of prices. The

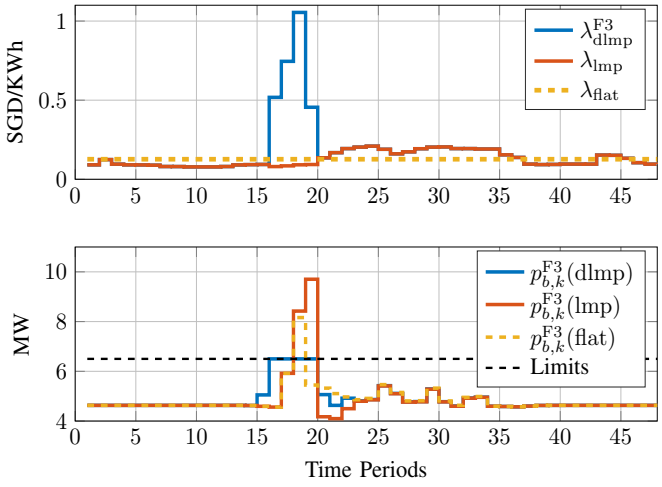

Fig. 2. Prices experience (top) and the resulting power flow across F3 (bottom).

price at the transmission-distribution grid interface is denoted as λ_{lmp}. The feed-in-tariff ($f_{0,k}$) used for selling energy back to the grid is assumed to be similar to λ_{lmp}. The mean value of λ_{lmp} is denoted by λ_{flat} and represented as the FT (see Section III). The optimal integrated price λ_{dlmp} is obtained from the procedure described in Section III. As an evaluation of pricing, first only power flow of F3 is presented in Fig. 2. From Fig. 2, it is obvious that with respect to adhering to the distribution grid branch flow constraints, λ_{dlmp} outperforms all other prices. This directly follows from (11), where the internal distribution grid constraints are included in the objective function of the optimization problem. In Fig. 3, scheduling of flexible loads and PV production of LP16 is presented. In general, for all three cases, due to the starting of occupancy periods, an increase in the scheduled consumption is observed during period 18-20. For the case of λ_{lmp}, optimization avoids a high price period (20 onwards), which results in an even higher consumption during period 18-20. This deviation in optimality is also observed in PV scheduling, where it's not economical anymore to cover the building's heating demand from the PV. As a result, PV production is fed back to the grid during periods (20-24). The scheduling due to the price λ_{dlmp} only differs from λ_{flat} when distribution grid constraints are binding. The scheduling result for the whole network is

Table I
Scheduling Results

Case	Peak Load (MW)	Losses (MW)	$p^{l}_{pv_{i,k}}$ (kWh)	$p^{g}_{pv_{i,k}}$ (kWh)	Cost (SGD)
λ_{flat} (1)	48	1.7	12	0.5	8275
λ_{lmp} (2)	54.3	6.1	9.9	2.6	8288
λ_{dlmp} (3)	46.3	3.4	11.4	1.2	8830

presented in Table I. To keep the notation compact, simulation results from λ_{flat}, λ_{lmp} and λ_{dlmp} are referred as case 1, 2 and 3. Due to flat price, the most cost effective scheduling is observed for case 1. The cost depreciation of 0.1% and 6% is observed for case 2 and 3, respectively. Please note that the total cost is lowest for case 1. However, compared to

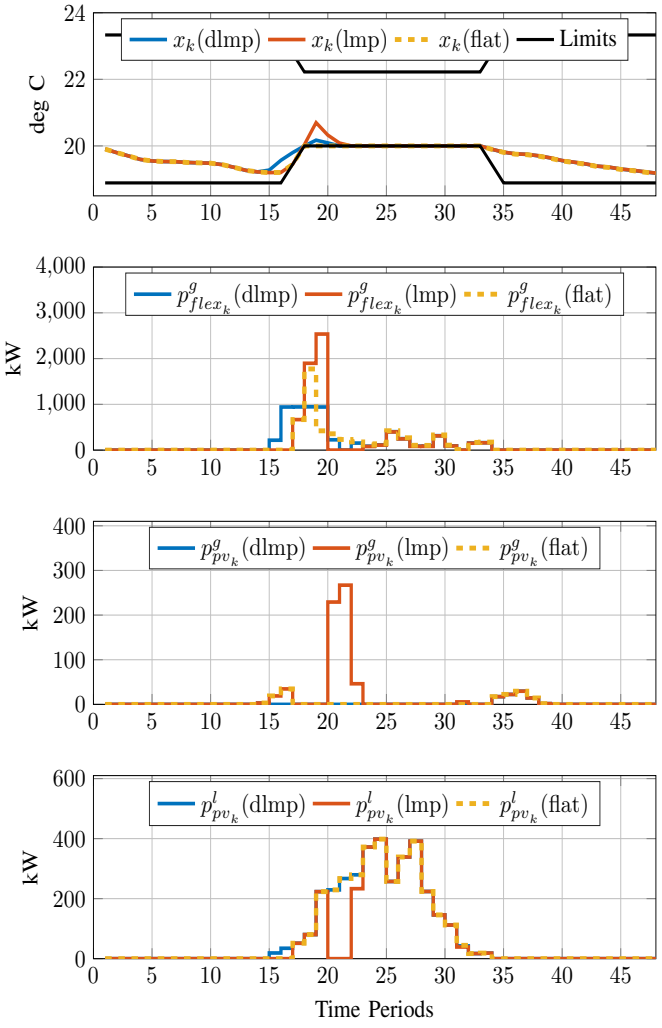

Fig. 3. Temperature evolution of one of the floor located at LP16 of F3 (top). Flexible load scheduled by LP16 (second from top). PV power sent back to the grid (second from bottom). PV power locally consumed within LP16 (bottom).

case 3, the peak load experienced by the grid is 3.7% higher in case 1. And as explained above, due to avoidance of high price period, the maximum (out of all cases) peak load of 54.3 MW is observed for case 2. Numerical results prove that case 3 presents the best pricing structure to reflect distribution grid constraints. However, it may not be the "ideal" candidate for the overall cost minimization of the flexible node injections. Similar conclusions are drawn with respect to PV power scheduling. The local PV power scheduling ($p^l_{pv_{i,k}}$) in case 1 again shows the best performance, whereas its value decreases by 17.5 and 5% in case 2 and 3, respectively. The PV feed-in power sent back to the grid experiences a similar trend. Please note that in this paper, even though no uncertainty in the PV production is assumed, it can still be observed that varying PV power feedback is experienced by the grid. As evident from Table I, a pricing structure (case 3) tailored to accommodate PV production and grid operation constraints achieves a good balance between a pure cost optimal demand response strategy (case 1 and 2). As a comparison, it can be

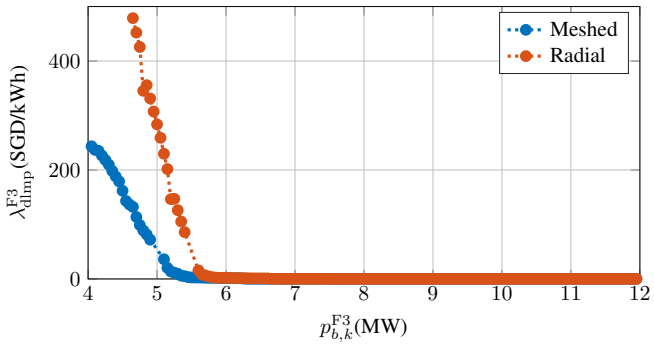

Fig. 4. Experienced prices and feasible power flows across F3 for both meshed and radial networks.

observed that, with respect to adhering to the distribution grid constraints, the optimal integrated pricing (case 3) outperforms other pricing structures (case 1 and 2).

B. Topology Comparison

In distribution grids, the possibility exists to operate it as a meshed network. Mostly, these networks are found in the urban environment. Since large commercial consumers are assumed to be operated as flexible loads, an analysis with respect to meshed topology of the distribution grid is also required. The network shown in Fig. 1 can be operated in a meshed structure by closing switches (SW1-4). Fig. 4 shows the effect on the integrated optimal price (λ_{dlmp}) and the feasible power flow ($p^{F3}_{b,k}$) experienced by F3. It can be observed that the feasible power flow increases in the meshed grid. Furthermore, the price experienced by F3 is also lowered for the meshed topology. This is due to the higher routing option in the case of the meshed network. In general, a drastic increase in the experienced price is observed close to the lower feasibility branch flow limits; approx. 4-5 MW for the meshed and 4.5-5.5 MW for the radial network. This information is very interesting for load operators, since in the end they have to bear the imposed cost. As explained above, the grid

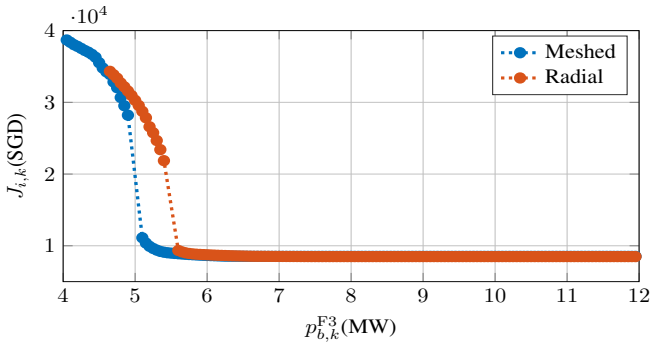

Fig. 5. The total cost of energy procurement and feasible power flows across F3 for both meshed and radial networks.

flexibility with respect to feasible branch flows increases in the meshed grid. This flexibility comes at a cost of a higher

overall increase in the cost of energy procurement. This effect can be observed in Fig. 5. The reason for a higher cost is due to the fact that even though the rerouting option makes the branch flow in one feeder feasible, it pushes the branch flows of other feeders to their respective limits. However, for the feasible power flow for both the meshed and radial network, the consumption cost for the meshed grid descends faster and saturates earlier than the radial grid. This effect is again explainable from the fact that the power transfer/shifting capability of the meshed network is higher than the radial one.

V. Conclusion & Future Work

In this paper, a generic cost optimal DR strategy with respect to various price signals and grid topology is evaluated. First, from simulation results, it is shown that integrating optimal pricing outperforms conventional pricing structures. Second, the influence of the changing topology of the distribution grid with respect to integrated optimal pricing is demonstrated. Results show that internal distribution grid constraints, when reflected in the prices, obtain a grid-friendly DR strategy. Furthermore, the meshed topology has the ability to host a higher amount of demand flexibility. But, this flexibility comes at a higher cost of energy procurement. The other downside of the meshed topology with the flexible demand is the distribution of the DLMP within various nodes of the distribution grid. This aspect has not been discussed in this paper, and we will intend to pursue it in our future work. Other tasks, such as investigating the information exchange and handling of the uncertainty in price and load dynamics, must also be investigated in the future.

VI. Acknowledgment

This work was financially supported by the Singapore National Research Foundation under its Campus for Research Excellence And Technological Enterprise (CREATE) programme. This work was also sponsored by National Research Foundation, Prime Ministers Office, Singapore under its Competitive Research Programme (CRP grant NRF2011NRF-CRP003-030, Power grid stability with an increasing share of intermittent renewables (such as solar PV) in Singapore).

References

[1] J. Torriti, M. G. Hassan, and M. Leach, "Demand response experience in Europe: Policies, programmes and implementation," *Energy*, vol. 35, no. 4, pp. 1575–1583, 2010.

[2] Federal Energy Regulatory Commission, "Assessment of Demand Response and Advanced Metering," Federal Energy Regulatory Commision, Tech. Rep., 2015. [Online]. Available: http://www.ferc.gov/legal/staff-reports/2015/demand-response.pdf

[3] N. Oconnell, P. Pinson, H. Madsen, and M. Omalley, "Benefits and challenges of electrical demand response: A critical review," *Renew. Sustain. Energy Rev.*, vol. 39, pp. 686–699, 2014.

[4] J. M. Morales, A. J. Conejo, H. Madsen, P. Pinson, and M. Zugno, *Integrating Renewables in Electricity Markets*, ser. International Series in Operations Research & Management Science. Boston, MA: Springer US, 2014, vol. 205.

[5] A. Zahedi, "Solar photovoltaic (PV) energy; latest developments in the building integrated and hybrid PV systems," *Renew. Energy*, vol. 31, no. 5, pp. 711–718, 2006.

[6] M. Maasoumy, A. Pinto, and A. Sangiovanni-Vincentelli, "Model-Based Hierarchical Optimal Control Design for HVAC Systems," *ASME 2011 Dyn. Syst. Control Conf. Bath/ASME Symp. Fluid Power Motion Control. Vol. 1*, pp. 271–278, 2011.

[7] F. Oldewurtel, A. Parisio, C. N. Jones, D. Gyalistras, M. Gwerder, V. Stauch, B. Lehmann, and M. Morari, "Use of model predictive control and weather forecasts for energy efficient building climate control," *Energy Build.*, vol. 45, pp. 15–27, feb 2012.

[8] D. B. Crawley, J. W. Hand, M. Kummert, and B. T. Griffith, "Contrasting the capabilities of building energy performance simulation programs," *Build. Environ.*, vol. 43, no. 4, pp. 661–673, apr 2008.

[9] Y. Ma, F. Borrelli, B. Hencey, B. Coffey, S. Bengea, and P. Haves, "Model Predictive Control for the Operation of Building Cooling Systems," *IEEE Trans. Control Syst. Technol.*, vol. 20, no. 3, pp. 796–803, 2012.

[10] V. et. al. Evangelos, "Robust Provision of Frequency Reserves by Office Building Aggregations," in *19th IFAC World Congr.*, B. Edward, Ed., Cape Town, aug 2014, pp. 12 068–12 073.

[11] S. Hanif, D. Fernando, M. Maasoumy, T. Massier, T. Hamacher, and T. Reindl, "Model predictive control scheme for investigating demand side flexibility in Singapore," in *2015 50th Int. Univ. Power Eng. Conf.*, 2015, pp. 1–6.

[12] G. T. Heydt, B. H. Chowdhury, M. L. Crow, D. Haughton, B. D. Kiefer, F. Meng, and B. R. Sathyanarayana, "Pricing and control in the next generation power distribution system," *IEEE Trans. Smart Grid*, vol. 3, no. 2, pp. 907–914, 2012.

[13] R. Verzijlbergh, L. J. De Vries, and Z. Lukszo, "Renewable Energy Sources and Responsive Demand. Do We Need Congestion Management in the Distribution Grid?" *IEEE Trans. Power Syst.*, vol. 29, no. 5, pp. 2119–2128, 2014.

[14] S. Huang, Q. Wu, S. S. Oren, R. Li, and Z. Liu, "Distribution Locational Marginal Pricing Through Quadratic Programming for Congestion Management in Distribution Networks," *IEEE Trans. Power Syst.*, vol. 30, no. 4, pp. 2170–2178, jul 2015.

[15] R. Li, Q. Wu, and S. S. Oren, "Distribution Locational Marginal Pricing for Optimal Electric Vehicle Charging Management," *IEEE Trans. Power Syst.*, vol. 29, no. 1, pp. 203–211, jan 2014.

[16] F. Li and R. Bo, "DCOPF-based LMP simulation: Algorithm, comparison with ACOPF, and sensitivity," *IEEE Trans. Power Syst.*, vol. 22, no. 4, pp. 1475–1485, 2007.

[17] G. Heydt, "The Next Generation of Power Distribution Systems," *IEEE Trans. Smart Grid*, vol. 1, no. 3, pp. 225–235, 2010.

[18] P. Sánchez-martín, "Modeling Transmission Ohmic Losses in a Stochastic Bulk Production Cost Model." [Online]. Available: http://www.iit.upcomillas.es/aramos/papers/losses.pdf

[19] O. W. Akinbode and K. W. Hedman, "Fictitious losses in the DCOPF with a piecewise linear approximation of losses," *IEEE Power Energy Soc. Gen. Meet.*, no. 5, 2013.

[20] D. Kirschen and G. Strbac, *Fundamentals of power system economics*. John Wiley & Sons, 2004.

[21] Energy Market Authority, "Introduction to the National Electricity Market," Energy Market Authority, Singapore, Tech. Rep. October, 2010. [Online]. Available: https://www.ema.gov.sg/cmsmedia/Handbook/NEMS{_}111010.pdf

[22] "Energy Market Company Singapore." [Online]. Available: https://www.emcsg.com/

[23] T. K. Kristoffersen, K. Capion, and P. Meibom, "Optimal charging of electric drive vehicles in a market environment," *Appl. Energy*, vol. 88, no. 5, pp. 1940–1948, 2011. [Online]. Available: http://dx.doi.org/10.1016/j.apenergy.2010.12.015

[24] "Solar Energy Research Institute for Singapore (SERIS)." [Online]. Available: http://www.seris.sg/

[25] R. Allan, R. Billinton, I. Sjarief, L. Goel, and K. So, "A reliability test system for educational purposes-basic distribution system data and results," *IEEE Trans. Power Syst.*, vol. 6, no. 2, pp. 813–820, 1991. [Online]. Available: http://ieeexplore.ieee.org/lpdocs/epic03/wrapper.htm?arnumber=76730